Analysis and Fabrication of Thick Co-cured Composite Structures

Zeaid Hasan[a], Jessica Rader[a], Delphine Turpin[a], Alec Olson[a], Ryan St Onge[a], Jon Amback[a]

[a]General Atomics Aeronautical Systems, Inc., Poway, CA, USA, 92064

ABSTRACT

Over the past decade advances in the design, materials, and manufacturing of thermoset composite materials have expanded rapidly. Nonetheless, aerospace structures have not yet adopted many of these technologies. This can be attributed to the risk averse nature of the engineering community and associated regulatory agencies in this field.

One of the technologies that has recently gained more traction is the use of unitized co-cure structures. Driving this change is the potential for reducing part count, touch time and labor costs. Most of the work to date focuses on thinner structures (~0.15 inch in thickness) resulting in a lack of work on much thicker parts representing wing-like structures.

This study sheds light on a recent large scale wing skin demonstrator built to understand the behavior of a thick co-cure stiffened wing skin. Details regarding the tooling concept, lamination and process development as well as post cure behavior will be discussed.

Keywords: co-cure, materials, composites, aerospace, analysis, cure cycle

Abbreviations

OML: Outer Mold Line
IML: Inner Mold Line
FEM: Finite Element Modeling
PW: Plain Weave
8HS: Eight Harness Satin Fabric
UD/UNI: Unidirectional
LM: Lamination Mold
DOC: Degree of Cure
DOF:Degree of Freedom
AFP: Automatic Fiber Placement
BUP: Build-up
CAD: Computer Aided Design
SFP: Sacrificial Plies
QTY: Quantity
DFM: Design for Manufacturing

1. INTRODUCTION

The use of composite materials in the industry primarily the aerospace and automotive has been expanding for the past four decades. Their superior properties such as light weight and high strength make them an attractive candidate to metallic materials such as titanium and aluminum.

The early use of composites in the aerospace industry was mainly for secondary non-structural applications such as fairings and flight control surfaces [1]. Given the tight regulatory nature of the aerospace industry, many certification and compliance details needed to be addressed prior to expanding the use of these materials across the airframe knowing that these regulations are constantly changing to ensure the safety of the general public [2]. Nowadays, the use of composites in both commercial and military airframes exceed 40% and are used for primary load path parts. That shift was possible due to the dedication of the industry to this innovation and the constant maturity in the analysis, material and process techniques as well as the fabrication approaches. Figure 1 shows examples of products that have used composites structures extensively in their platform.

Figure 1. Products that use composite materials in parts of their structure

The main cost drivers when it comes to composites is the raw material, tooling, labor, manufacturing process, production volume and equipment. Any improvements in those areas has the potential to drive the cost down. With the advances occurring in those areas over the next few decades the cost of building parts from composites is believed to become more competitive with metallic materials which will make them an even larger competitor when it comes to future products [3].

From the manufacturing point of view, composites offer the unique ability compared to other materials of formability. Designs that would have never been thought possible using aluminum for example are now possible. Co-curing has been the strength of composites and presents the best way of combining various parts without fasteners. Since the different parts are concurrently formed and bonded to each other, the assembly stresses are avoided. The reduction in number of parts results in reduced number of fasteners and reduced assembly cycle. Figure 2 shows a comparison between a structure where you co-cure the different components together to make one part without the need to use any mechanical fasteners and the fastening approach.

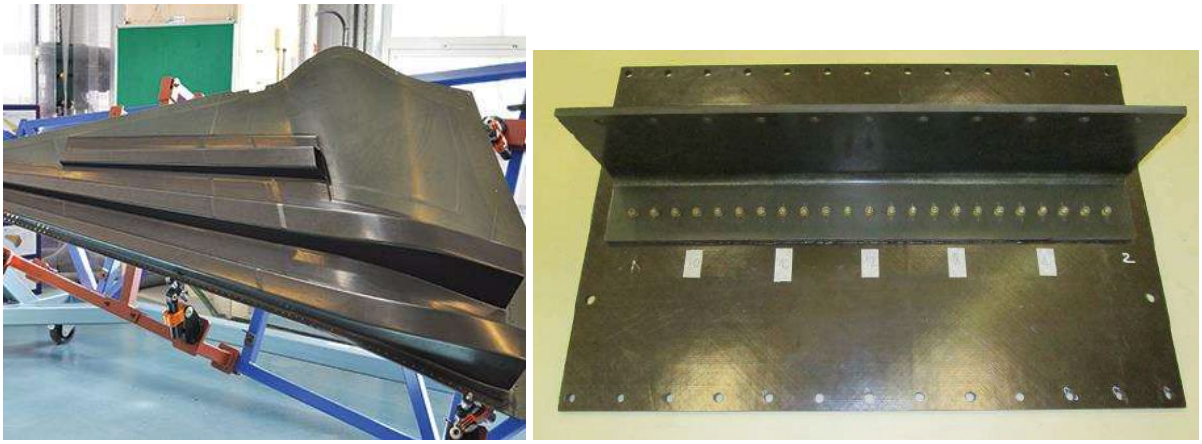

Figure 2. Comparison between a) co-cured structure b) fastened structure

Many different designs have been proposed in the literature when it comes to composite parts [4-9] but few have ever taken those concepts and built parts to evaluate the proposed designs. It has been shown that co-cured structures compared to co-bonded structures have a more complex failure mode and are shown to be superior to bonded parts in many cases [10]. To ensure that the final co-cured part is well designed, a great deal of interaction between the design and fabrication teams is required. The final configuration of such parts should be decided based on its structural and fabrication feasibility [11].

When it comes to large primary structural parts (e.g wings) there is always the need to add stiffening features to improve on their stability and strength. There are many different kinds of such stiffeners that have been widely used in the industry and each type behaves in a unique manner. Blade stiffeners are one type that have a great deal of use and many have evaluated their performance in detail [12] but the fabrication aspect is considered to be more complex compared to other options. Hat-shaped stiffeners are another widely considered stiffening feature typically used in aerospace parts. They are generally easier to build compared to blades including I shaped stiffeners. The co-cure of those stiffeners to the mating structure is also shown to be less susceptible to structural delamination compared to others [13].

In this study we will be using Hat stiffeners for the evaluation in addition to an out of autoclave material system namely Cycom 5320-1. Although it has been shown that using a fully out-of-autoclave (OoA) process is feasible for composites [14] we elected to use an autoclave for the cure process given the thickness of the part. Many studies have shown that using an autoclave process for curing thermoset materials is superior to many other alternatives that have been evaluated [15]. The primary reason for using this material system was the high open hole compression (OHC) allowable values compared to other conventional material systems widely used in the aerospace industry (e.g 977-2) which is considered the driving allowable for part sizing. It is important to note that having any defect in the part will cause a knockdown to that allowable. A decrease in compressive strength was noticed with an increase in defect

height [16] which emphasizes the importance of nondestructive inspection to ensure the part is free of defects post cure.

In this paper we will present details on the analysis and fabrication of large co-cure composite structures. The manufacturing aspect including pre and post analysis will be presented and lessons learned will be provided in order to enable the use of integrated composite structures more rapidly in the future.

2. DESIGN

The study focuses on aerospace structures namely wing skins given their need for stiffening features to enhance their structural integrity. A high-level overview of the size of the wing skin demo is shown on Figure 3.

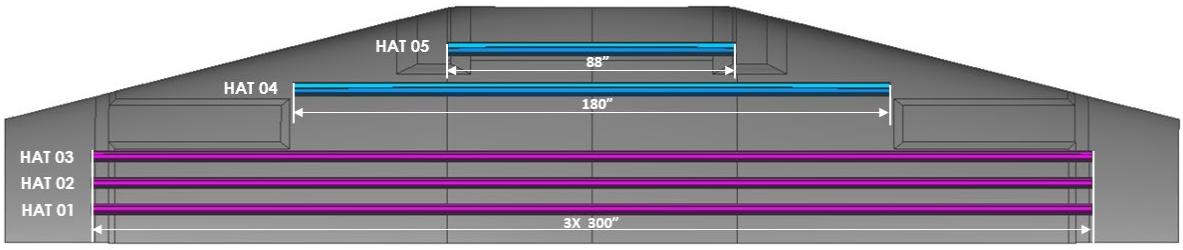

Figure 3. Wing skin demo design outline

In order to understand the different variables that will impact the quality of the part build we incorporated as many of those variables from the actual wing design into the demo wing skin design. Those variables can be summarized as follows:

Hat stiffener size: two primary sizes were used in the demo. The first was approximately one inch tall and another that was two inches tall while they both incorporate similar stacking sequence to eliminate that as a variable. The level of complexity in fabricating each type was of interest to the team in order to provide feedback as part of the design for manufacturing (DFM) feedback.

Hat mandrel type: two primary types of mandrels were used for the build. For the smaller size compression molded mandrels were used. Those are known to exhibit less expansion under temperature which is preferred to minimize the part distortion during cure. The other was an extruded mandrel and those have larger expansion but are known to be less expensive and have a quicker procurement time. Summary of both can be found in Table 1.

Table 1. Mandrel types used on the wing skin demo

MANDREL TYPE 1	MANDREL TYPE 2
Compression Molded Mandrel • Silicone (350°F rated) • FEP coating (from manufacturer) • 25-ft (qty 3) 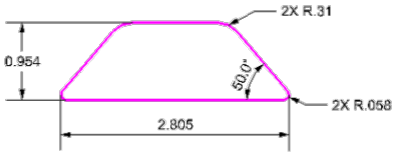	**Extruded Mandrel** • Silicone (250°F rated) • Wrap with Teflon tape (done in-house) • 15-ft (qty1), 7.3-ft (qty 1) 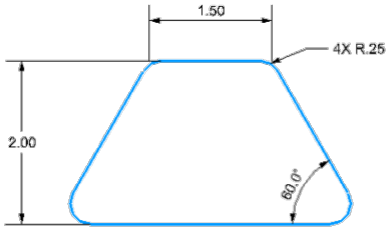

Laminate thickness: since the actual design will incorporate many different laminate build-ups (BUPs) and thicknesses across the part we decided to include some of those details in the demo to evaluate the performance and identify shortfalls of any specific detail that needed attention. The skin thickness ranges from 0.5 inches to 0.3 inches which depends on the level of ply BUPs used in a specific region as shown in Figure 4. A unique stacking sequence was used for the hats and were consistent among all 5 hat stiffeners.

Tooling material: in this study we used a composite tool that included a curvature that is more extreme compared to the actual design to ensure we capture all the complexities. The tooling material was LTM45 and the lamination mold (LM) was scanned prior to any lamination to ensure it is within the engineering tolerances of +-0.015 inch across the part.

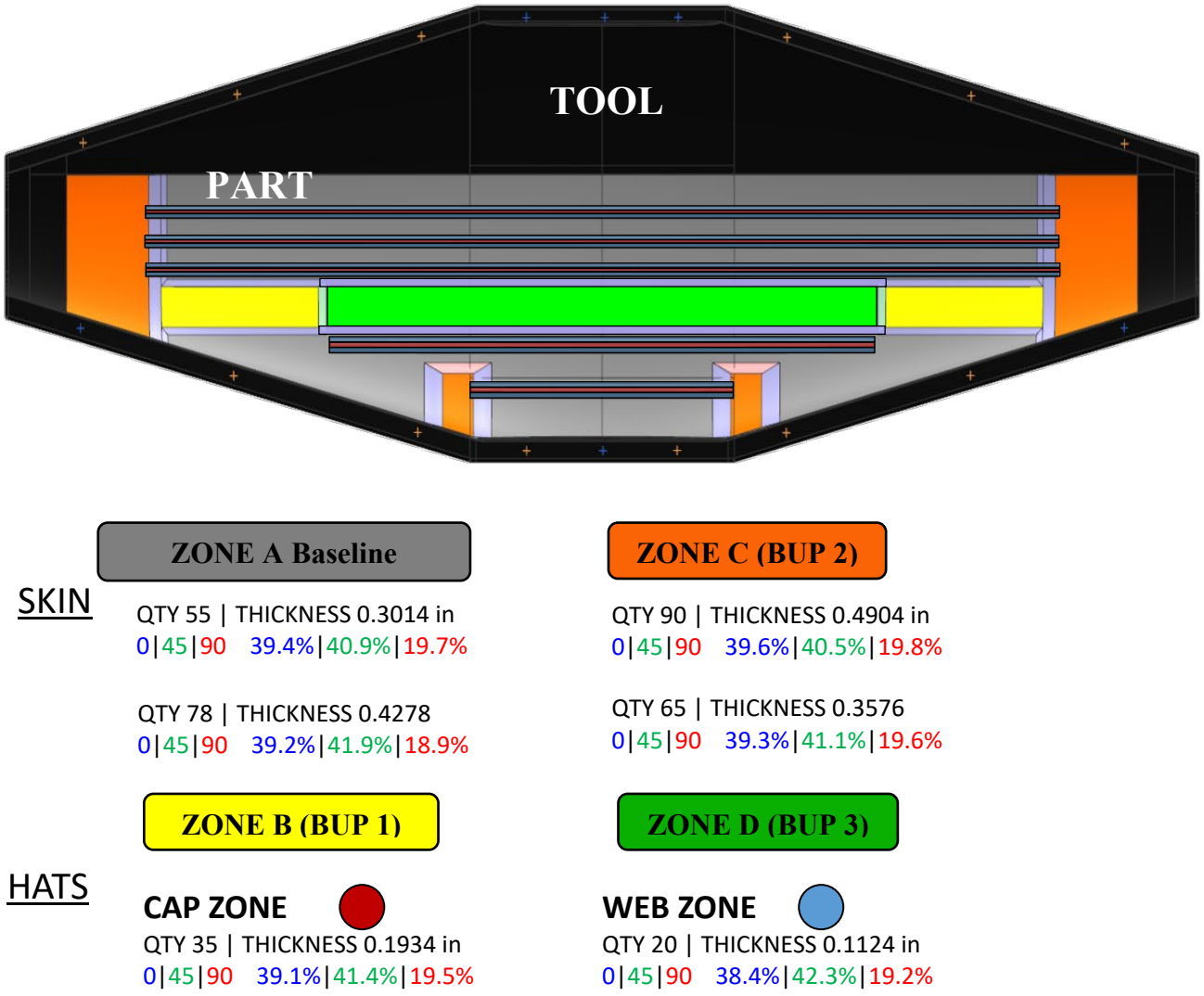

Figure 4. Skin and hat stacking sequence in the different regions of the wing demo

Sacrificial plies: Another variable that will be evaluated in this demo is the use of sacrificial plies for the purposes of machining post cure.

In order to ensure that the part is within the engineering tolerances post cure, the part is machined to fit the CAD model. The location where those sacrificial plies were included is shown in Figure 5. Those areas typically correspond to joints where spar and rib interface exist. In an ideal world there will be no need for sacrificial plies as the part should be fabricated per the design requirements but given the thermal gradients during cure, the unsymmetric and unbalanced behavior of the laminate, and the geometric differences across the part, those factors all lead to the creation of residual stresses within the part impacting the part warpage. In addition, human error and other material inconsistencies cause the part to lie outside engineering and design boundaries adding to the need for sacrificial plies. If one was able to prevent those factors we can envision a time where the use if sacrificial plies is eliminated.

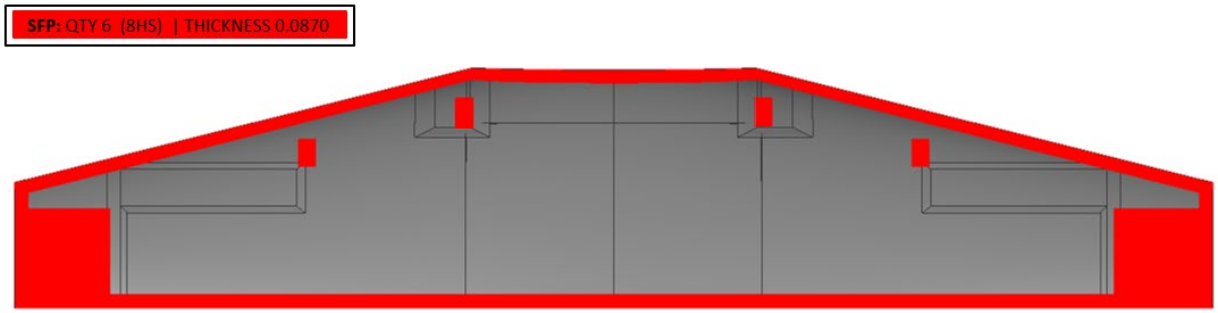

Figure 5. Sacrificial ply locations used across the wing skin demo

Tow filler: The tow filler is used to fill the gap that is created when laminating the hat stringers as shown in Figure 6. It is well known that the filler is considered a critical structural integrity and final quality of that part [17-20]. Hence, additional focus needs to be given to the fabrication process of this feature in order to reduce any anomalies that can impact its quality. We used two different materials for the evaluation, adhesive rolls made from FM309-2 and unidirectional Cycom 5320-1 with T650 fibers using a proprietary fabrication method. Both types will be evaluated as part of this demo.

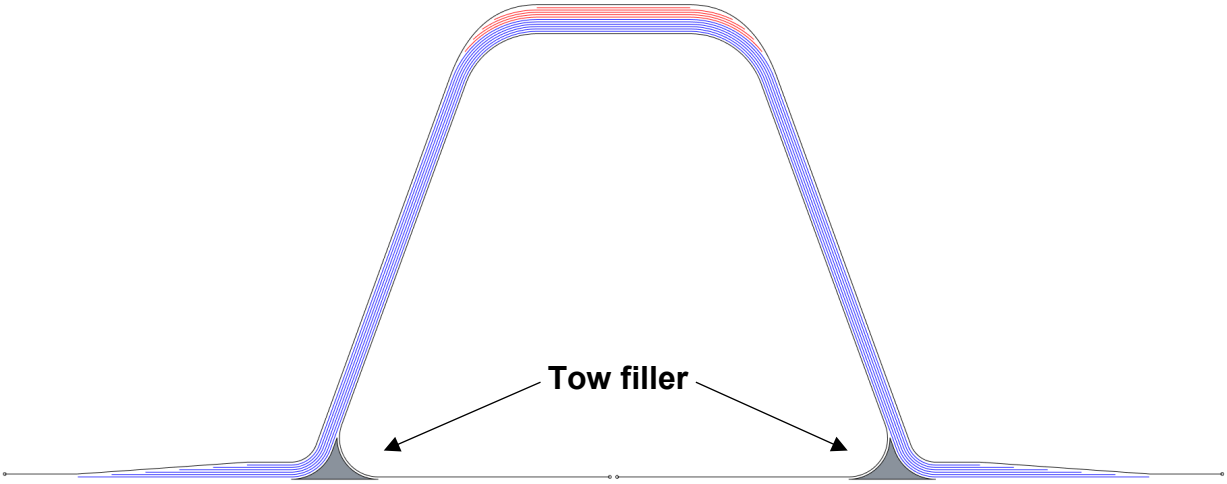

Figure 6. Tow filler used during the fabrication of composite hat stringers

3. FABRICATION

The fabrication process utilized hand-layup as the primary method of lamination since it was considered our baseline process for building the part during production. This study will allow the development team to capture any critical details that need to be adjusted in the process specification prior to building the production parts. A high-level overview of the lamination process is shown in Figure 7.

Figure 7. Overview of the lamination process used for the wing skin demo

The skin included 55 plies overall with the addition of 35 plies in the build-up regions. The thickness was 0.3 inches with a max thickness near build up regions of 0.5 inch. The overall stacking sequence was a 40/40/20 laminate design utilizing all unidirectional material form. Plain weave was used as cover plies on the OML and IML surface of the skin and 8HS material form for the sacrificial plies.

FiberSim [21] was used to perform the ply splicing for this effort. The total number of individual plies was more than 1300 which is considered to be a very large number by all standards. Therefore, the handling of that many ply quantities as well as ensuring that the material out-time is not exceeded (20 days for handling and 30 days while on tool under vacuum) was a critical requirement. During the layup it was noted that the ±45°ply orientation which had a size 42 inch wide x 98 inch long was manageable to handle with minimal issues overall. The same applied to the 90°ply orientation of size 42 inch wide x 70 inch long. On the other hand, the 0°ply orientation size 42 inch wide x 200 inch long caused difficultly during layup in the form of wrinkles. Figure 8 shows the lamination of the wing skin excluding the hat stiffeners.

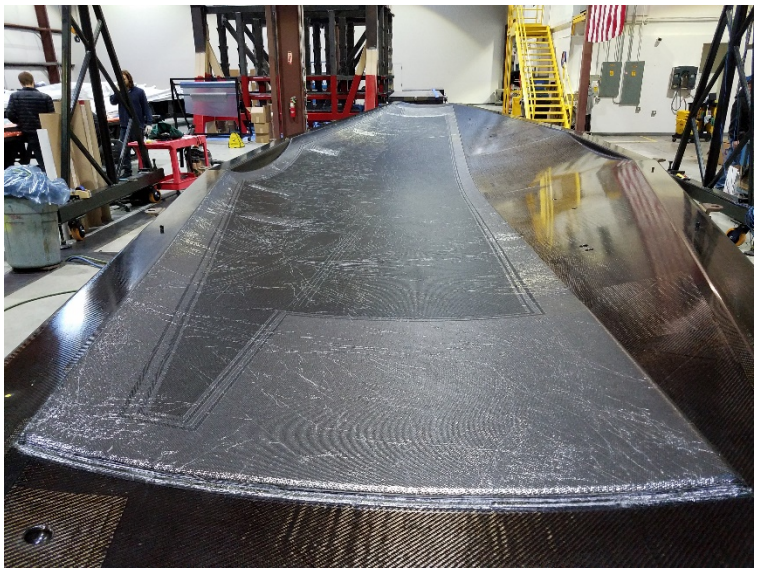

Figure 8. Final wing skin lamination

The hat stringers had a total of 35 plies with thickness of 0.2 inch (20 web plies and 15 cap plies). We used rubber mandrels from Rubbercraft, LLC, as the preferred product for this demo. The lamination occurred

one ply at a time using hand layup. A similar 40/40/20 laminate design was used with all unidirectional material form for the exception of PW cover plies on mandrel and IML surface. In order to ease the post cure inspection specifically the blue light scanning to measure the movement of the hats pre and post cure a pre-impregnated peel ply (P15448) was used on the IML side.

Some of the challenges that were observed during lamination can be summarized below:

- Compound curvature induced wrinkles in 0°skin plies
- Demo utilized maximum material width of 43 inch which was difficult to handle
- Working out wrinkles was difficult and time consuming
- Inability of FiberSIM to predict the wrinkles in the part using the set threshold values.

Improvement opportunities:

- Adjust FiberSIM properties for unidirectional material
- Splice material to smaller widths
- Provide manufacturing training to increase familiarity with FiberSIM generated ply kits on the floor

Once the skin was fully laminated, the hat mandrels with the initial wrap ply had to be transferred on in the appropriate location per design requirements. For this demo the mandrel was placed on an FEP layer and wood support for transport. Laser projections were made on the skin and the tool was transferred near those laser points as shown in Figure 9. Footprint projection were used for initial placement and centerline projection were used for final quality assurance (QA) verification. Mandrel centerline was hand-marked onto a wrap ply after poly removal. The FEP was then carefully pulled out from under the mandrel and the mandrels carefully moved back to center line. Mandrels were taped in place to reduce mandrel movement during debulk which was done after all the hats were placed in position. It was noted that the mandrels were slightly raised above part surface at the BUP ramp locations prior to debulk. An approximate gap of 0.125 inch was seen but after debulk the gap closed with no issues.

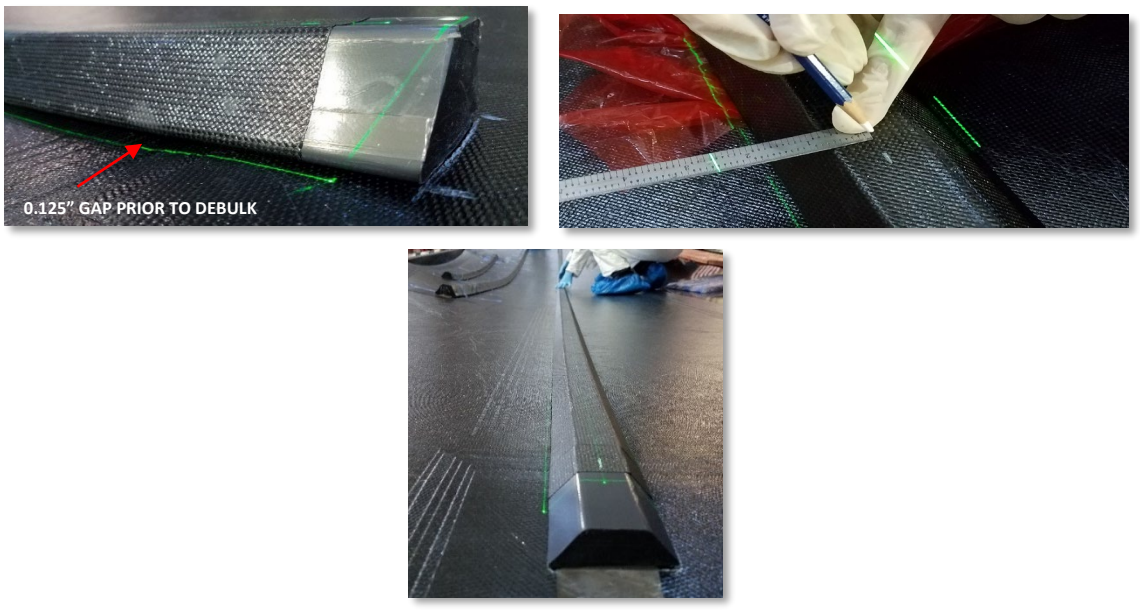

Figure 9. Mandrel placement during the wing skin demo fabrication

After the five hats were placed we finalized the lamination process by dropping the tow fillers. As stated earlier, two material systems were use, pre-formed UNI tows on HAT 04, HAT 05 which were five feet in

length as shown in Figure 10. The tow filler conformed to the tool curvature with no heat required. Teflon tools used to secure tows into the mandrel radius. Hand rolled adhesive film were used on HAT 01, HAT 02, HAT 03. Material strips were folded into ¼" strips on a heated table and then rolled to final shape. HAT 01 had a 1.0" wide strip while HAT 02, HAT 03 had a 1.5" wide strip. Tows were heated with a heat gun and formed into mandrel radius using Teflon roller. The final wing skin is shown in Figure 11.

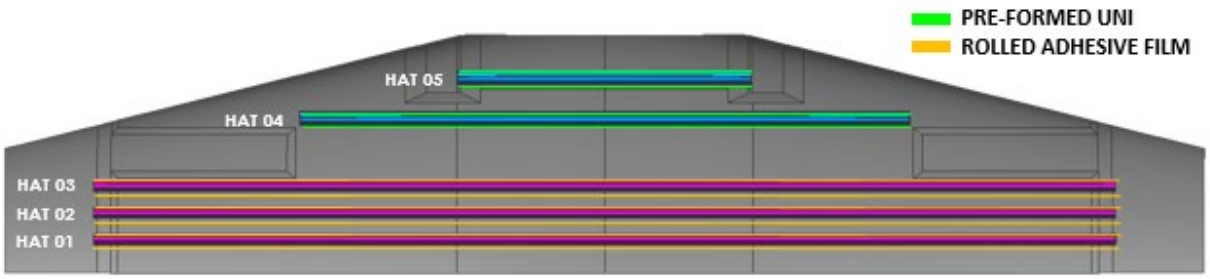

Figure 10. Tow filler types used on the wing demo

Figure 11. Final wing skin part

After the completion of the lamination process comes the need to perform the appropriate bagging to prevent any leakage during cure. Bag leakage is a well-known nonconformance that typically occurs during the manufacturing process and might cause the part to get scrapped [22] which begs the need for investigation prior to building parts in production. Given the sheer size of the full scale demo, unique challenges were identified that needed to be addresses and documented for inclusion in the process specification.

In addition, since this is a fully co-cure process and given the thickness changes across the part an uncontrolled exotherm could cause the panel to cure from the inside out, causing severe process-induced residual stresses. To prevent that, detailed evaluation of the cure cycle and temperature distribution should be captured to understand the thermal gradients observed in the part and provide a recommendation on the final cure prior to production build. As noted previously the material that is used in this study for fabricating the part is Cycom 5320-1 epoxy resin system with T650 fibers. Given the large thickness of the part we needed to ensure first that we have a cure cycle that will lead to a fully cured high quality part. RAVEN software [23] currently has this material system fully characterized and we took advantage of that fact to evaluate many cure cycles and come up with an ideal case for the specific details pertaining to this demo. Figure 12 shows a specific cure cycle and the corresponding degree of cure (DOC) which reaches an appropriate value which provided us with enough confidence to pursue this cure recipe for the demo part.

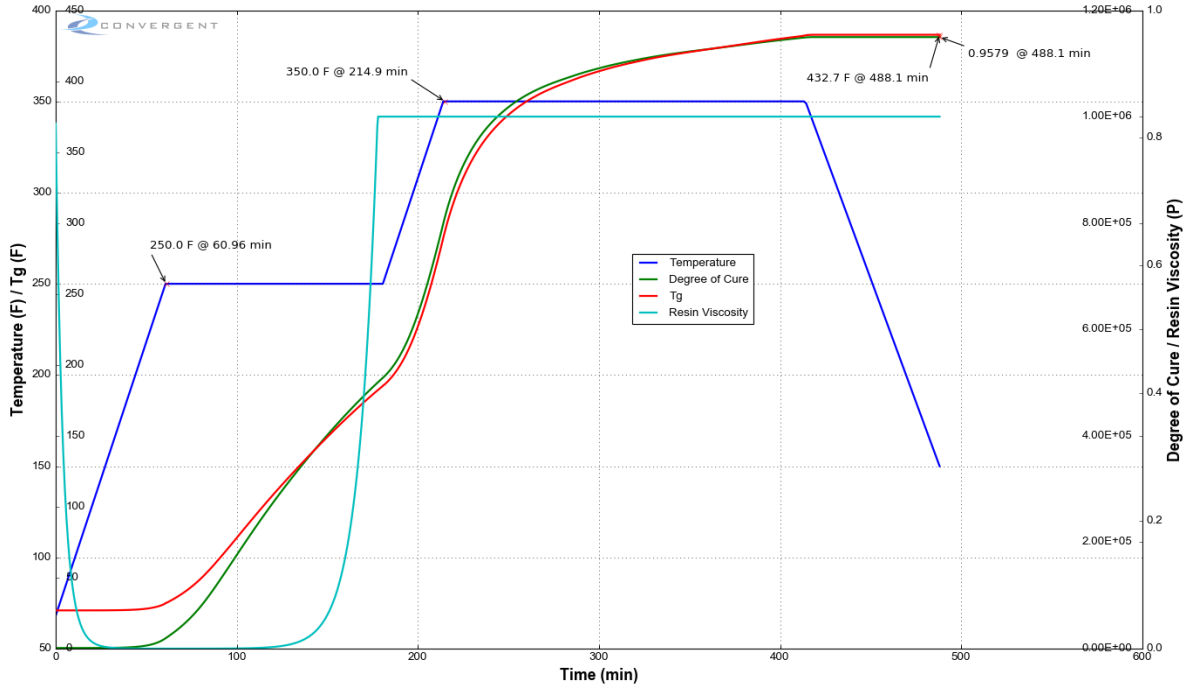

Figure 12. Cure cycle analysis for Cycom 5320-1

4. RESULTS

In order to quantify the amount of movement the hat stiffeners observed after cure, a pre-cure and post-cure scan of the demo was taken using blue light technology and analyzed the level of displacement as shown in Figure 13. It is extremely important to ensure that the movement does not exceed the values set by engineering as the parts may not be able to fit during assembly (e.g rib onto the skin). The engineering tolerance set for this study was a nominal sealing gap between the rib and hat of 0.140".

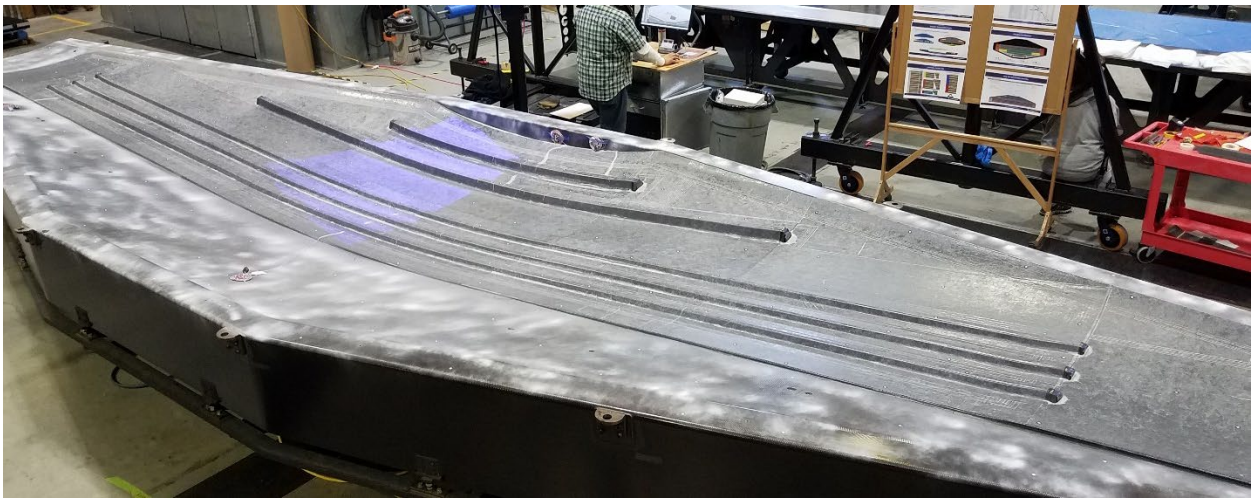

Figure 13. Blue light used to measure the part deformation pre-cure and post-cure

The comparison was done between the post cure part and the CAD model design which ideally should be within the set engineering tolerances. Figure 14 shows that comparison, note that the scan was taken while the part was still on the tool and vacuum applied to eliminate any residual stress effects on the measurements.

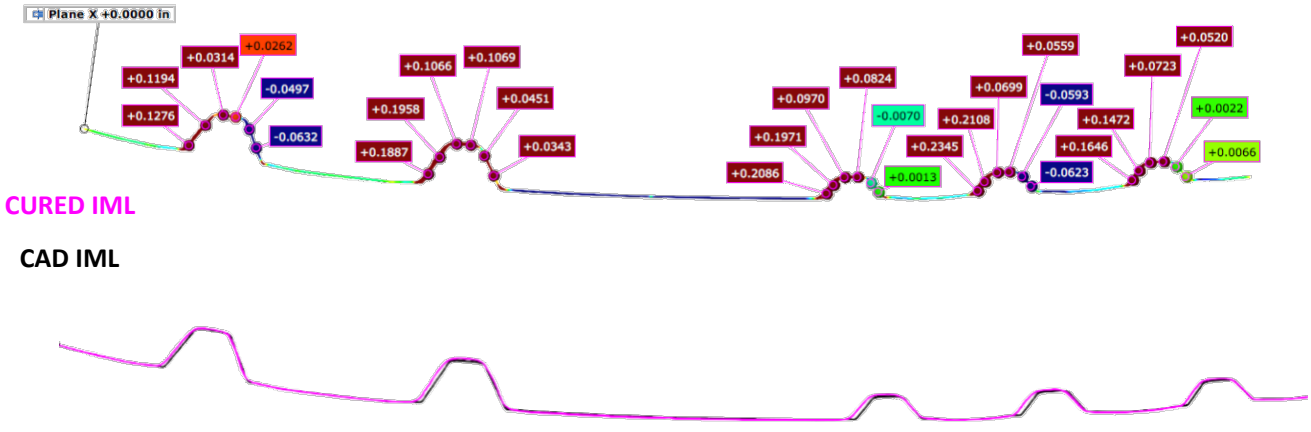

Figure 14. Post cure comparison to the CAD model

The max profile deviations of the hat stiffeners was approximately +0.208” but for the majority of the part the deviation was within the engineering tolerances set. There are several potential reasons for the excessive movement in those areas. One of those can be attributed to the blue light scan data which has potential inaccuracies in the best fit process. Another is the deviations due to the initial placement of the hat stringer onto the skin. Recall that the hat stringers were placed based on a laser projection and that may have caused errors in placement. One remedy to this issue can be the additional use of tooling or shop aides required for mandrel positioning. An additional reason for the deviation can be attributed to the mandrel expansion. Depending on the type of mandrel, the expansion ranges up to 5% for the extruded mandrel on each web wall and up to 3.5% for the compression molded mandrel on each web wall. Figure 15 shows a scan of a hat stiffener and comparison to the CAD surface post cure. As shown, the mandrel expansion impacts the final shape of the part across the perimeter. Finally, since the CAD model does not account for mandrel expansion we can expect some differences due to that when performing the comparison.

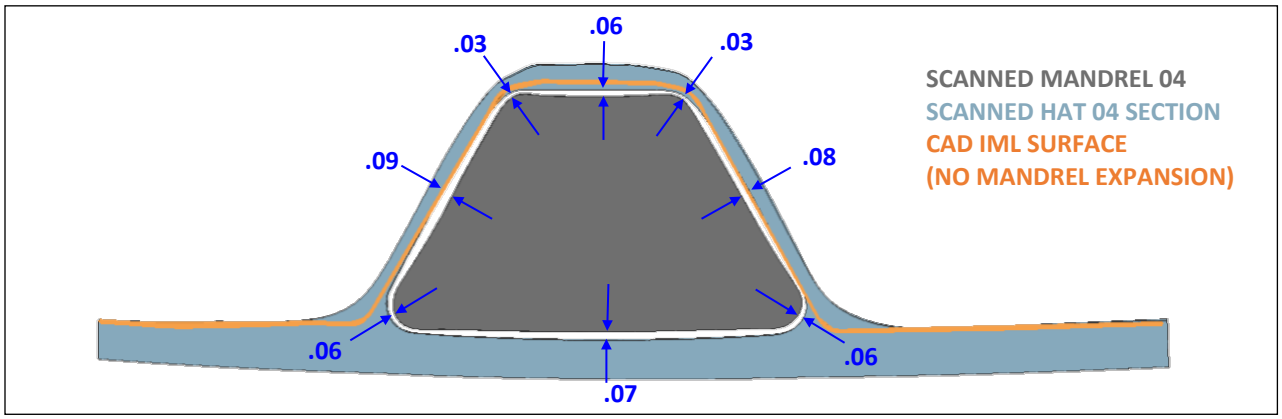

Figure 15. Mandrel expansion effect on the final part shape

Another part of the evaluation was the nondestructive inspection. A C-scan of specific critical areas in the part was done in order to identify the part quality and ensure it is free of defects. Given the lack of large scale equipment to scan the entire part and time associated with that the focus was only on areas of concern related to the design. Those areas included the hat terminations, large curvature regions, locations where wrinkles were seen during layup, build-up regions and ply drop terminations near hat web plies. Figure 16 shows the areas where the scan was taken and the corresponding results.

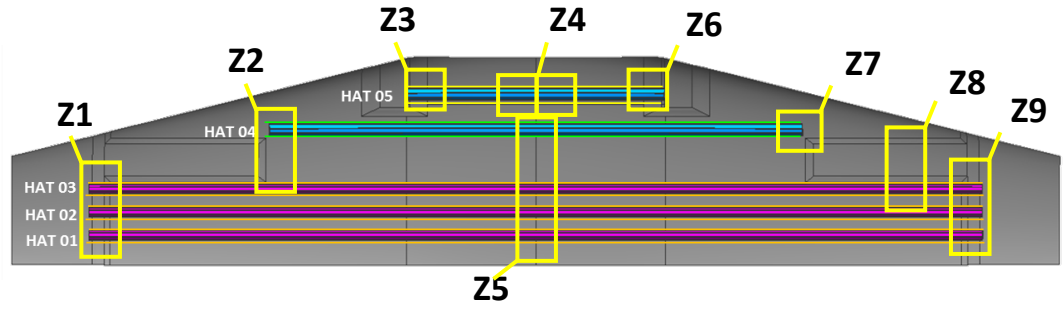

Figure 16. Nondestructive inspection results of the wing skin demo

It can be noted that zone 1 included inter-laminar indications within the skin over the tow area while zone 2, 7 and 9 had minimal inter-laminar indications. Zone 3 shows some indications near the hat termination. In order to correlate those indications to a level of damage or porosity destructive inspection was conducted. Figure 17 shows a cross section cut near Zone 2 and the level of porosity seen in that region. As shown, the porosity level was less than 0.1% which is much lower than the threshold specification limit of 2%.

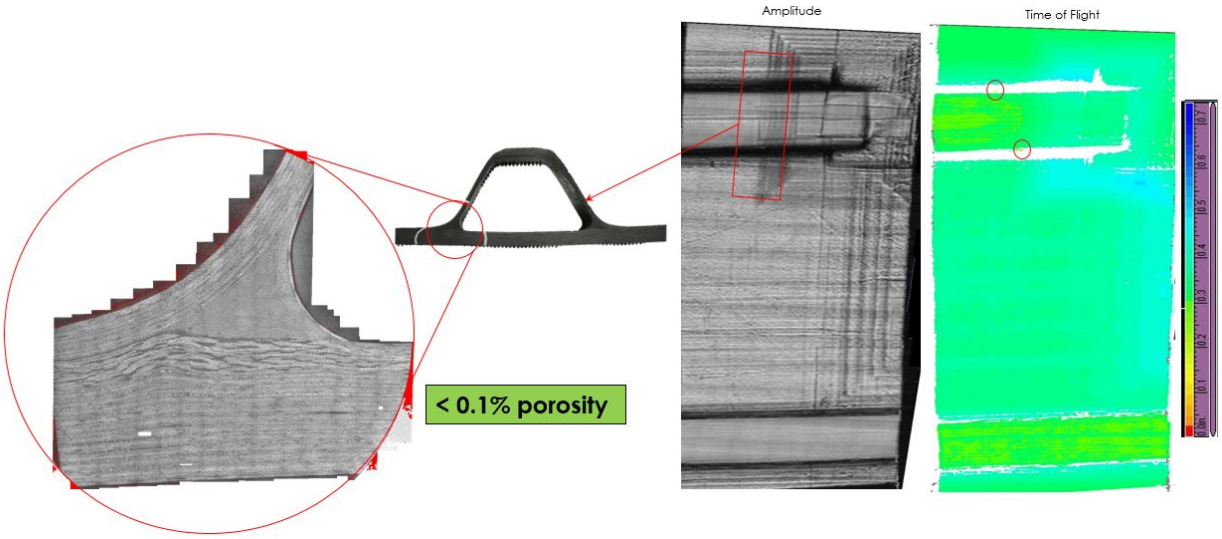

Figure 17. Micro-section cut of Zone 2 to correlate NDI with porosity

5. ANALYSIS

When it comes to composite structures it is well known that having an anisotropic laminate creates thermal strains and residual stresses causing the part to warp. From that perspective the phenomena can be prevented by striving for a symmetric layup during the design phase. For curved sections however, differences in strains through-thickness, in-plane direction and geometry will result in a change in part shape which came to be known as spring-back as shown in Figure 18.

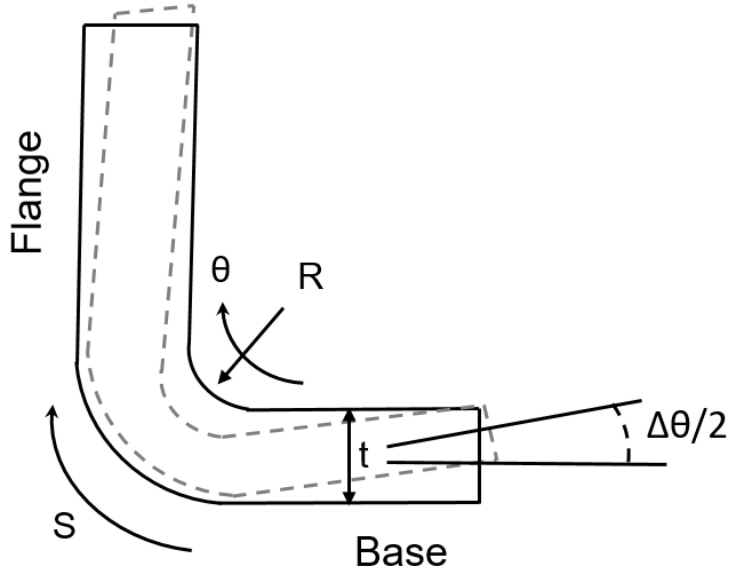

Figure 18. A schematic representation of the spring-back phenomena in composite structures

The first attempt to calculate the magnitude of the spring-back angle was proposed by Nelson and Cairns [24] using the following equation:

$$\Delta\theta = \theta\left[\frac{(\alpha_{\theta-}\alpha_R)\Delta T}{1+\alpha_R\Delta T}\right] \quad (1)$$

where θ is the angle between the base and flange, $\Delta\theta$ is the change in the angle between the pre-cure and post-cure state, α_θ is the laminate thermal expansion coefficient in the circumferential direction, α_R is the laminate thermal expansion coefficient in the radial direction and ΔT is the temperature change.

When it comes to thin components the through-thickness variations in temperature and resin degree of cure are usually very small and their contribution to the residual stress build-up and deformation may be neglected. In thicker parts however, the low composite transverse thermal conductivity coupled with the rapid heat generation of the resin reaction may result in significant temperature and cure gradients. Those gradients are potential sources of residual stresses in the part. In addition, if the boundary conditions during processing are not symmetric due to presence of process tooling an asymmetric stress state may develop resulting in warpage. The uneven resin flow also results in uneven thermal and cure shrinkage strains. These strains result in non-uniform residual stress states and warpage in the part. The tool also plays a role in the residual stress formation through the influence of temperature and mechanical loads and constraints applied at the tool part interface.

The impact of many of these variables have been studies by many researchers [25-27] and they have shown the importance of understanding those details during the preliminary design phase in order to reduce their impact on the final product. However, there is lack in evaluating thick co-cured stiffened structures in the literature which is one of the objectives of the current study.

When it comes to thermoset materials the stiffness of the resin significantly depends on the degree of cure and can be defined as [28]

$$E_r = (1 - \alpha_{mod})E_r^0 + \alpha_{mod}E_r^\infty + \gamma\alpha_{mod}(1 - \alpha_{mod})(E_r^\infty - E_r^0) \quad (2)$$

$$\alpha_{mod} = \frac{\alpha_\theta - \alpha_{mod}^{gel}}{\alpha_{mod}^{diff} - \alpha_{mod}^{gel}} \quad (3)$$

where E_r^0 and E_r^∞ are the fully uncured and fully cured resin moduli, respectively. α_{mod}^{gel} and α_{mod}^{diff} are the bounds on the degree of cure during the phase when the resin modulus is assumed to develop and γ is a parameter representing the competing mechanisms between stress relaxation and chemical hardening [28]. Generally, it is assumed that E_r^0 is equal to $E_r^\infty/1000$ as a first approximation [28].

When it comes to the geometry of the part and since we are dealing with stiffened structures the details of the design will have a large impact on the warpage as well. Assume that we select a representative element from the wing skin and we divide it into beams based on the unique features it exhibits as shown in Figure 19. Each beam will have its own behavior based on its characteristics but due to the need for continuity in traction and displacement at the interface [30] that will cause some asymmetry in the overall behavior which reflects on the warpage seen in the part.

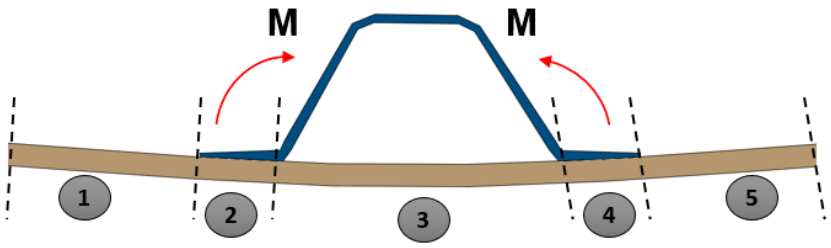

Figure 19. Representative section of a stiffened hat structure

And since we are dealing with thick structures the bending moment adheres to the following equation [31]

$$M = \frac{\Delta\theta}{\theta}ER_n(RA_m - A) = \frac{\Delta\theta}{\theta}E\frac{t}{ln\left(\frac{R_0}{R_i}\right)}\left(\left(R_i + \frac{t}{2}\right)bln\left(\frac{R_0}{R_i}\right) - bt\right) \quad (4)$$

where t is the beam thickness, E is the elastic modulus, b is the element width and R is the radius of curvature. In this study we will use the commercial FEM software Abaqus to simulate the cure behavior of the part to quantify the amount of warpage. In order to accurately model the material behavior, the plug-in COMPRO will be utilized [29] that uses a modified approach to defining the material kinetics incorporating the temperature dependency as suggested in the CHILE approach [25]. Note that Cycom 5320-1 was fully characterized and available for use in this plug-in. The model used 8-node linear brick, incompatible mode C3D8I as the element type. The total degree of freedom (DOF) of the model was approximately 10 million with a runtime of 8hrs using 8cpus on a supercomputer. The skin and hat stacking sequence mapped that of the actual design. An overview of the model is shown in Figure 20.

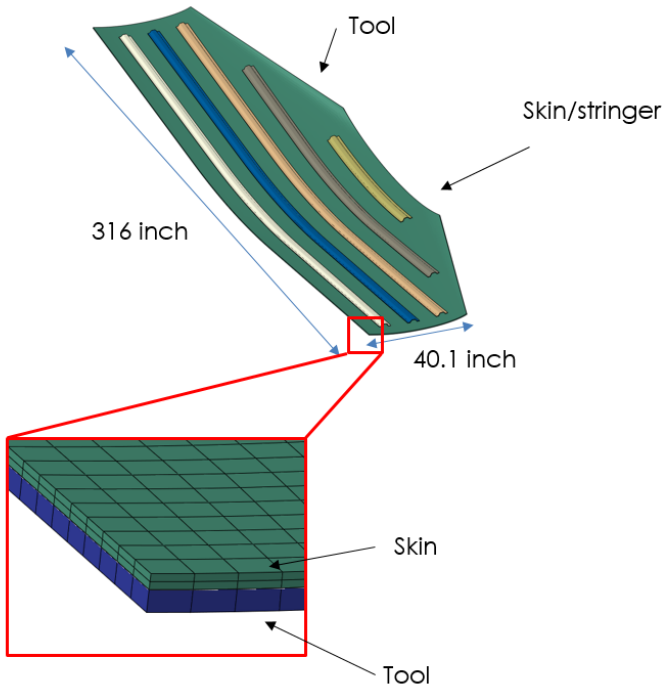

Figure 20. Finite element model details

First a comparison was made between the warpage measurements taken from the wing demo and the FEM model when the part was demolded while remaining on the tool. Several data points were measured around the periphery as shown in Figure 21 and the correlation among the points was within 33% at the corners and generally within 50% elsewhere. Note that the simulation utilized similar boundary conditions to ensure that the behavior is captured as accurately as possible. The deviation can be explained by the movement of the part during the de-bagging process. Overall, the simulation provided an accurate representation of the part behavior post cure. Figure 22 shows the part warpage when the part was removed from the tool and assuming no gravity effects on the part. As shown, the part max displacement was 0.507 inches and it was shown that the part can be positioned back to its nominal shape while applying vacuum to the part causing minimal structural concerns. This demo provided insight to the flexibility into the co-cure structure compared to a co-bonded part where the later will require additional force to pull the part back to nominal shape causing the need to consider warpage more closely. The hypothesis behind this behavior in the co-bonded structure stems from the larger reaction forces caused by the cured stringers onto the un-cured skin during the second curing phase which translates into added residual stresses and hence warpage.

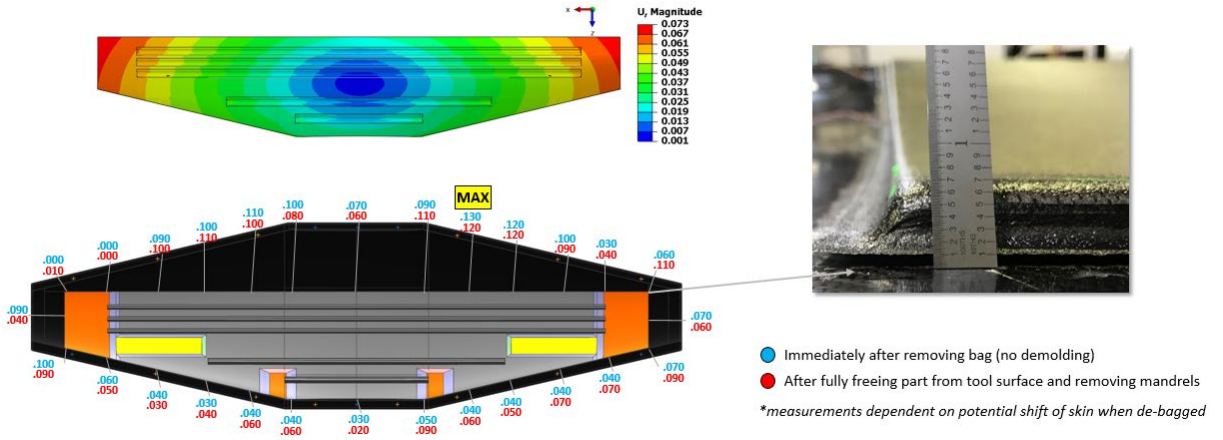

Figure 21. Correlation between the model and the experimental results for the part prior to transferring it fully from the tool

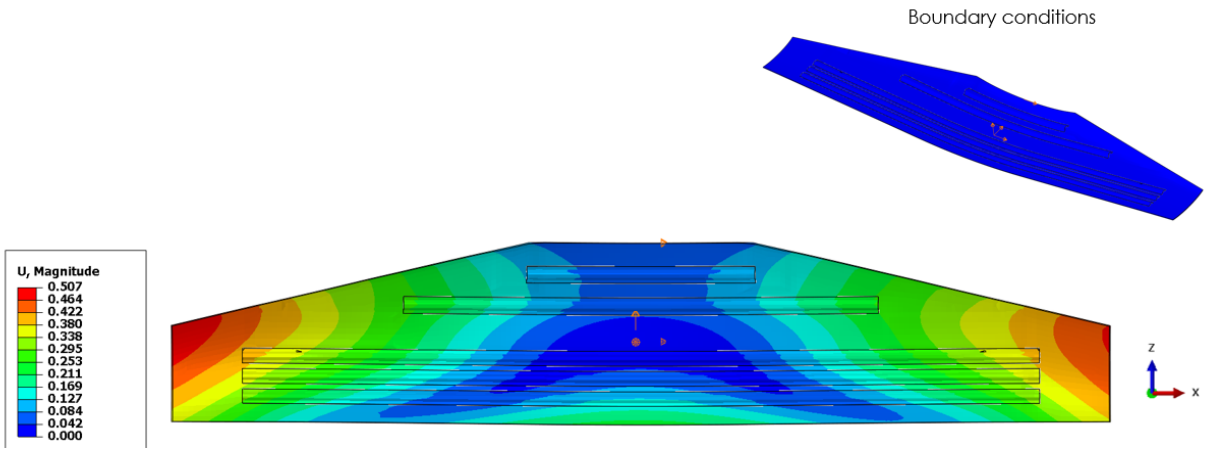

Figure 22. Part displacement post-cure with no gravity effects on the part

6. CONCLUSION

This paper discussed the analysis, design and fabrication of a thick wing skin demo. Several variables were considered during the build including the tooling approach, mandrel type, tow filler material, hat size and sacrificial ply materials. It was shown that the use of a compression molded mandrel was superior to that of the extruded type due to the reduced thermal expansion it exhibits. One change to the mandrel design should be the inclusion of a hole in order to further reduce that expansion and the associated hat stiffener bowing. The proposed hat shape moving forward shall adhere to that shown in Table 2.

Table 2. Hat stringer sizes used in the wing skin demo

PROPOSED MANDREL TYPE
Compression Molded Mandrel with Hole • Silicone (350°F rated) • FEP coating (from manufacturer) 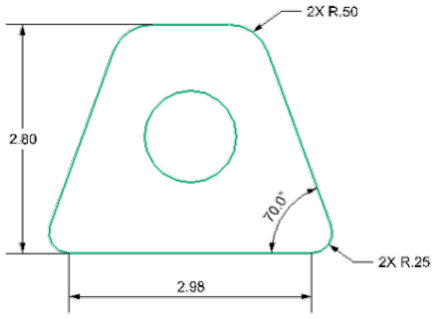

The use of 8HS material form as sacrificial plies was shown to generate bow waves near the tow filler region of the hat and it's recommended to replace it with unidirectional material form in order to minimize that effect. It was also shown that the use of shim material near the termination of the hat in order to support the removal of the mandrel post cure is mandatory as the lack of it will cause imprints and bow waves as well.

The post cure inspection showed minimal anomalies in the destructive and nondestructive testing ensuring that the fabrication approach will be able to build a satisfactory part that adheres to engineering requirements. Even though the part did not fully adhere to the location requirements per the measurements taken it is believed that with the use of the updated mandrel type and reduction in thermal expansion will lead to better values closer to that set by engineering.

Acceptable correlation was shown among the FEM and the fabricated part when it came to the warpage measurements. The overall behavior was captured effectively. It was found that the warpage in thick co-cure structures was less than that in the co-bonded process which provides designers with the need to consider this effect depending on the fabrication approach.

7. REFERENCES

[1] Kumara, M., et al. 2012, “Fractographic Analysis of Tensile Failures of Aerospace Grade Composites” Materials Research. 2012; 15(6): 990-997

[2] Schmid, T., et al, 2015, “Bonding of CFRP primary aerospace structures – discussion of the certification boundary conditions and related technology fields addressing the needs for development” Composite Interfaces 22(8):795-808

[3] Rao, S., et al, 2018, “Carbon Composites are Becoming Competitive and Cost Effective” Infosys white Paper

[4] Allen, G., Belisario, D., 2004, “Co-cured composite structures and method of making them” US Patent US6743504B1

[5] Simpson, C. et al, 2010, “Single piece co-cure composite wing” US Patent Application US20060249626A1

[6] Stephens, J. et al 2012, “Method and Apparatus for Co-Curing Composite Skins and Stiffeners in an Autoclave” US Patent Application US20140096903A1

[7] Biornstad, R., 2004, “Composite barrel sections for aircraft fuselages and other structures, and methods and systems for manufacturing such barrel sections” US Patent US7527222B2

[8] Humfeld, K., Nelson, K., 2015, “Co-curing process for the joining of composite structures” US Patent US9731453B2

[9] Hasan, Z., et al, 2018, “Unitized Composite Structure Manufacturing System” US Patent Application

[10] Abliz, D., et al, 2013, “Mixed-mode fracture toughness of co-cured and secondary bonded composite joints” Polymers and Polymer Composites 21(6):341-348

[11] Gaddikeri, K., Rao, M., 2002, “Co-curing Techniques for Integrally Stiffened Shells” Conference Paper · January 2002

[12] Huang, C., 2003, “Study on co-cured composite panels with blade-shaped stiffeners” Composites Part A Applied Science and Manufacturing 34(5):403-410

[13] Kim, G., et al, “Manufacture and performance evaluation of the composite hat-stiffened panel” Composite Structures Volume 92, Issue 9, August 2010, Pages 2276-2284

[14] Centea, T., et al, 2015, “A review of out-of-autoclave prepregs – Material properties, process phenomena, and manufacturing considerations” Composites Part A: Applied Science and Manufacturing Volume 70, March 2015, Pages 132-154

[15] Geissberger, R., et al, 2017, “Rheological modelling of thermoset composite processing” Composites Part B: Engineering Volume 124, 1 September 2017, Pages 182-189

[16] Davidson, P., Waas, A., 2017, “The effects of defects on the compressive response of thick carbon composites: An experimental and computational study” Composite Structures Volume 176, 15 September 2017, Pages 582-596

[17] Hasan, Z., 2014, "An investigation into the performance of composite hat stringers incorporating nanocomposites using a multiscale framework" Journal of Reinforced Plastics and Composites, Vol 33, Issue 15.

[18] Hasan, Z., Chattopadhyay, A., 2013, "Thermo-Mechanical Analysis of Structural Elements Incorporating Nanocomposites" ASME 2013 International Mechanical Engineering Congress and Exposition Volume 9: Mechanics of Solids, Structures and Fluids

[19] Hasan, Z., et al, 2014, "Multiscale approach to analysis of composite joints incorporating nanocomposites" Journal of Aircraft 52 (1), 204-215

[20] Hasan, Z., et al, 2019, "Design, Analysis and Fabrication of Thick Co-cured Wing Structures" Composites Part B, In Review.

[21] https://www.plm.automation.siemens.com/global/en/products/nx/fibersim.html

[22] Price, T., 1997, "Handbook: Manufacturing Advanced Composite Components for Airframes" U.S. Department of Transportation, FAA.

[23] https://www.convergent.ca/products/raven-simulation-software

[24] Nelson RH, Cairns DS (1989) Prediction of dimensional changes in composite laminates during cure. 34th International SAMPE symposium and exhibition, vol 34, pp 2397–2410

[25] Johnston, A., 1997, "An Integrated Model of the Development of Process-Induced Deformation in Autoclave Processing of Composite Structures" Thesis

[26] Zobeiry, N., et al. 2003, "Efficient Modelling Techniques for Predicting Processing Residual"

[27] Padovec, Z., 2012, "Springback analysis of thermoplastic composite plates" Applied and Computational Mechanics 6 (2012) 25–34

[28] Bogetti TA, Gillespie JW Jr (1992) Process-induced stress and deformation in thick-section thermoset composite laminates. J Compos Mater 26(5):626–660

[29] https://www.convergent.ca/products/compro-simulation-software

[30] Sadd, M, 2005, "Elasticity, Theory, Application and Numerics" Elsevier Butterworth Heinemann

[31] http://www.roymech.co.uk/Useful_Tables/Beams/Curved_beams.html